The results are shown in the last column of Table II.

One sees from Table II that $R(Cp) \gg R(Ph)$ at all temperatures, supporting the independent rotation of the cyclopentadienyl rings relative to the aryl ring. One would expect any steric interaction between the two rings to be reflected by an equivalent reduction in $R(Cp)$. From this result, the authors believe that one may reasonably eliminate steric hindrance as the basis of the observed phenyl rotation barrier in $Cp_2Co_2(CO)_4(CPh)$, which may, therefore, be attributed primarily to electronic orbital interactions between the bridging CO and capping phenyl group.[9,11-13]

Summary and Conclusions

In this investigation, we have utilized ^{13}C NMR spin-lattice relaxation times to obtain a complete characterization of the overall and internal rotation dynamics in $Cp_2Co_3(CO)_4(CPh)$ as a function of temperature in the solvent chloroform.

From the phenyl carbon T_1's, we obtained the molecular tumbling diffusion coefficient, $D_\perp$, and the *total* phenyl ring spinning rate, $D_S(Ph) = D_\parallel + R(Ph)$. $D_S(Ph)$ in the complex was found to be 1 order of magnitude lower than both (a) the equivalent rotational rate of free benzene in chloroform and (b) the measured values of $D_S(Ph)$ in $Co_3(CO)_9(\mu_3\text{-}CPh)$, a cluster with neither electronic nor steric interactions between the ring and molecular skeleton.

^{13}C relaxation times of the terminal carbonyl ligands, measured at two magnetic field strengths, were used to calculate the parallel diffusion constant, $D_\parallel$, of the cluster's framework. It was observed that, to within experimental error, $D_\parallel = D_S(Ph)$, from which it was concluded that the *internal* phenyl rotational rate, $R(Ph)$, is ~ 0 on a nanosecond time scale. This result permitted the determination of an estimated range for the barrier, V_0, to internal rotation: 5 kcal/mol $< V_0 <$ 9 kcal/mol.

To determine whether the hindrance to internal rotation of the phenyl group in the cluster might be due to a gear type mutual interaction of the phenyl and cyclopentadienyl rings, ^{13}C T_1's of the Cp carbons were used to calculate the internal rotation rate of this ring about its C_5 axis. It was found that $R(Cp) \gg R(Ph)$ at all temperatures, from which one may reasonably conclude that the barrier is not due to inter-ring steric effects. Rather, the rotational barrier can be attributed to electronic interaction of the bridging CO's π^* orbital with the aryl π system through the metal 2e orbitals, as proposed recently by Stone et al.[13] to explain the slowed ring rotation in $CoFe_2(\mu_2\text{-}CO)(CO)_8(\mu_3\text{-}CC_6H_4Me\text{-}4)$.

The results of this investigation illustrate the powerful utility of the NMR relaxation time technique to probe reorientational and internal rotation dynamics on a nanosecond time scale. In this system, these measurements permitted the observation and estimation of an internal rotation barrier which could not be detected by using conventional temperature-dependent ^{13}C NMR spectroscopy.

To the authors' knowledge, this is only the second metal carbonyl cluster in which an orbital interaction between a bridging CO and capping ligand has been observed experimentally and the first for which the barrier range to internal rotation has been determined. Further experiments on additional homo- and heteronuclear systems will be required to assess the generality and range of magnitudes of this type of electronic interaction.

Acknowledgment. We acknowledge the Robert A. Welch Foundation [Grants B-1039 (M.G.R.) and B-657 (M.S.)] and the UNT Faculty Research Fund for support of this research.

Contribution from the Department of Chemistry, University of Arizona, Tucson, Arizona 85721

Spectroscopic and Electrochemical Studies of Monomeric Oxomolybdenum(V) Complexes with Five-Membered Chelate Rings and Alkoxo or Alkanethiolato Ligands

Chaung-Sheng J. Chang and John H. Enemark*

Received July 12, 1990

A series of monomeric oxomolybdenum(V) complexes of the type LMoO[X-CHR'-CHR''-Y] (L = hydrotris(3,5-dimethyl-1-pyrazolyl)borate; X = O, Y = S, R' = Me, R'' = H or R' = R''= H, Me; X = Y = O, S, R' = R'' = Me) have been synthesized. Several monoalkoxo and monoalkanethiolato complexes with the general formula of LMoO(Cl)(XR) (X = O, R = Me, Et, ^{n}Pr; X = S, R = Et, ^{n}Pr, ^{i}Pr) also have been prepared. All of these complexes have been characterized by elemental analyses, mass spectrometry, infrared and UV-visible spectroscopy, electron paramagnetic resonance (EPR) spectroscopy, and cyclic voltammetry. The electronic absorption spectra for chelate complexes with X = Y = O or S show two transitions with similar extinction coefficients in the range 400-900 nm. The energy difference between these two bands is approximately 3400 and 3600 cm^{-1} for X = Y = O and S, respectively. In the potential window +2.0 to -2.0 V, all of these complexes exhibit one quasi-reversible reduction wave, corresponding to forming the analogous monooxomolybdenum(IV) species. The reduction potentials shift to the negative direction with an increase in the number of methyl groups on the chelate rings and with an increase in the number of methylene units in the monodentate alkoxo or alkanethiolato ligands.

Introduction

The molybdenum cofactor, Mo-co (I), is proposed to possess pterin and alkyl phosphate ester moieties that attach to a dithiolene group.[1,2] The actual functions of these groups in the side chains are not yet known, but the pterin group may be involved in electron transfer with the molybdenum center during turnover.[3]

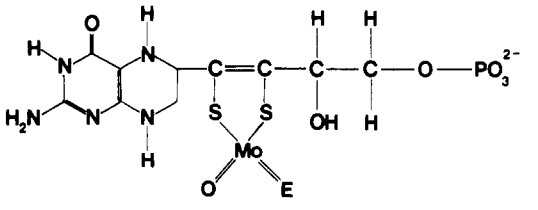

(E = O, S)

(I)

Recently, we have reported that the variation of the sizes of the chelate rings in a series of monomeric (diolato)- and (dithiolato)oxomolybdenum(V) complexes can have marked effects

(1) (a) Johnson, J. L.; Rajagopalan, K. V. *Proc. Natl. Acad. Sci. U.S.A.* **1982**, *79*, 6856-6860. (b) Kramer, S. P.; Johnson, J. L.; Riberiro, A. A.; Millington, D. S.; Rajagopalan, K. V. *J. Biol. Chem.* **1987**, *262*, 16357-16363.

(2) Cramer, S. P.; Stiefel, E. I. In *Molybdenum Enzymes*; Spiro, T. G., Ed.; Wiley: New York, 1985; Chapter 8, pp 411-441.

(3) (a) Burgmayer, S. J. N.; Stiefel, E. I. *J. Chem. Educ.* **1985**, *62*, 943-953. (b) Lehnen, J.; White, B. M.; Kendrick, M. J. *Inorg. Chim. Acta* **1990**, *167*, 257-259.

0020-1669/91/1330-0683$02.50/0

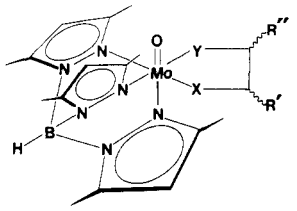

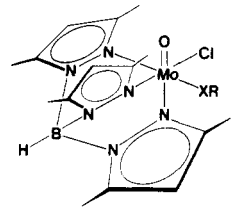

	X	Y	R′	R″
(1)	O	S	H	H
(2)	O	S	Me	H
(3)	O	S	Me	Me
(4)	O	O	Me	Me
(5)	S	S	Me	Me

	X	R
(6)	O	Me
(7)	O	Et
(8)	O	^{n}Pr
(9)	S	Et
(10)	S	^{n}Pr
(11)	S	^{i}Pr

Figure 1. Stereochemistry and abbreviations for complexes **1–11**.

on the electrochemical potentials and electronic transition energies.[4] For the chelated diolato and dialkoxo complexes, we also reported that the results from He I photoelectron spectroscopy (PES) in the gas phase are complementary to the measurements in acetonitrile solution and support the observed electrochemical behavior.[5]

Here, we extend our spectroscopic and electrochemical studies to a series of monomeric monooxomolybdenum(V) complexes containing five-membered chelate rings, which can be considered to be a simplified system for modeling the substituent effects on the chelate ring of Mo-co. Complexes with monoalkoxo or monoalkanethiolato ligands are also studied. These complexes allow us to investigate how the spectroscopic and electrochemical behaviors are perturbed by systematic variations of the ligand substituents (Figure 1).[6]

Experimental Section

Materials. Solvents were purified by distillation under an inert atmosphere of dry nitrogen as follows: acetonitrile and dichloromethane from calcium hydride; benzene by double distilling using a method suggested by Bercaw;[7] hexanes and pentanes from sodium hydride; tetrahydrofuran from potassium/benzophenone; toluene and triethylamine from potassium. Potassium hydrotris(3,5-dimethyl-1-pyrazolyl)borate (KL) and $LMoOCl_2$ were prepared according to previous methods.[8,9] Silica gel (70–230 mesh, pore diameter 60 Å) used in adsorption chromatography was obtained from Sigmal Chemical Co. The free acids of ligands were purchased from Aldrich Chemical Co and used without further purification. Tetra-*n*-butylammonium tetrafluoroborate was recrystallized several times from aqueous ethanol and dried at 120 °C in vacuo for 48 h before use. The reactions were carried out under an inert atmosphere of dry nitrogen by using standard Schlenk techniques; solvents were thoroughly degassed before use by repeated evacuation followed by admission of dry nitrogen. Subsequent workup was carried out in air. Elemental analyses were performed by Atlantic Microlab Inc., Atlanta, GA.

Preparation of Compounds 1–11. To a $LMoOCl_2$ solution (1.00 g, 2.08 mmol, in 200 mL of toluene or benzene) at 30 °C was slowly added either a mixture of 0.64 mL (4.6 mmol) of triethylamine and 2.3 mmol of appropriate chelate, alcohol, or thiol in 15 mL of toluene (or benzene) or a suitable amount of the potassium salt of the ligand, and this solution containing $LMoOCl_2$ and ligand was heated gradually to suitable reaction temperature (vide infra). The purity of isolated compounds as well as the progress of the reactions was monitored by thin-layer chromatography and EPR spectroscopy. Upon completion (6–8 h for **1–3** at 70–80 °C; 8 h for **4** at 65 °C; 24 h for **5** at 50 °C; 5 h for **6–8** at 70 °C; 12 h for **9–11** at 70 °C), the reaction mixture was cooled to room temperature, filtered, evaporated to dryness in vacuo, and chromatographed on a silica gel column. Purified compounds were stored in an inert-atmosphere box.

LMoO[O–(CH$_2$)$_2$–S] (1), LMoOCl(OMe) (6), and LMoOCl(SEt) (9) have been reported previously.[9] The data listed in Tables I–III are consistent with those in the literature.

LMoO[O–CH(Me)CH$_2$–S] (2). The crude product was dissolved in a minimum amount of benzene, and the solution was chromatographed on silica gel with benzene. The compound eluted as a dark green band, which was evaporated to dryness; the yield was 62%. Anal. Calcd for $C_{18}H_{28}BN_6O_2SMo$ (MW 499.27):[10a] C, 43.30; H, 5.65; N, 16.83; S, 6.42. Found: C, 44.98; H, 5.93; N, 16.09; S, 5.87. MS: *m/z* 498. IR: $\tilde{\nu}$(BH) = 2542 cm^{-1}, $\tilde{\nu}$(MoO) = 936 cm^{-1}.

LMoO[O–CH(Me)CH(Me)–S] (3). The purification method used for this compound was similar to that described for **2**. The yield was 74%. Anal. Calcd for $C_{19}H_{30}BN_6O_2SMo$ (MW 513.30):[10b] C, 44.45; H, 5.89; N, 16.37; S, 6.25. Found: C, 45.88; H, 5.82; N, 15.94; S, 5.99. MS: *m/z* 512. IR: $\tilde{\nu}$(BH) = 2542 cm^{-1}, $\tilde{\nu}$(MoO) = 935 cm^{-1}.

LMoO[O–CH(Me)CH(Me)–O] (4). The crude product was dissolved in a minimum amount of tetrahydrofuran, and the solution was chromatographed on silica gel with tetrahydrofuran–toluene (1:9 v/v). The compound eluted as a pale gray-blue band, which was evaporated to dryness. The residue was redissolved with a minimum amount of tetrahydrofuran, and the solution was added to 50 times this volume of stirring *n*-pentane; the solid was filtered out, washed several times with *n*-pentane, and dried in vacuo. The yield was 55%. Anal. Calcd for $C_{19}H_{30}BN_6O_3Mo$ (MW 497.23):[10c] C, 45.90; H, 6.08; N, 16.90. Found: C, 47.17; H, 6.43; N, 16.09. MS: *m/z* 497. IR: $\tilde{\nu}$(BH) = 2537 cm^{-1}, $\tilde{\nu}$(MoO) = 937 cm^{-1}.

LMoO[S–CH(Me)CH(Me)–S] (5). The crude product was dissolved in a minimum amount of benzene, and the solution was chromatographed on silica gel with benzene. The compound eluted as a dark brown band, which was evaporated to dryness; the yield was 83%. Anal. Calcd for $C_{19}H_{30}BN_6OS_2Mo$ (MW 529.35):[10d] C, 43.11; H, 5.71; N, 15.88; S, 12.11. Found: C, 45.34; H, 5.90; N, 14.98; S, 11.53. MS: *m/z* 530. IR: $\tilde{\nu}$(BH) = 2546 cm^{-1}, $\tilde{\nu}$(MoO) = 929 cm^{-1}.

LMoOCl(OEt) (7). The crude product was dissolved in a minimum amount of dichloromethane, and the solution was chromatographed on silica gel with dichloromethane–hexanes (2:1 v/v) as eluant. The compound was isolated as a pale green powder, washed with minimum *n*-hexane, filtered out, and dried. The yield was 95%. Anal. Calcd for $C_{17}H_{27}BClN_6O_2Mo$ (MW 489.64): C, 41.70; H, 5.56; N, 17.16; Cl, 7.24. Found: C, 41.71; H, 5.54; N, 17.07; Cl, 7.29. MS: *m/z* 491. IR: $\tilde{\nu}$(BH) = 2545 cm^{-1}, $\tilde{\nu}$(MoO) = 947 cm^{-1}, $\tilde{\nu}$(MoCl) 337 cm^{-1}.

LMoOCl(O^{n}Pr) (8). The purification process for this compound is similar to that for compound **7**. The yield was 66–74%. Anal. Calcd for $C_{18}H_{29}BClN_6O_2Mo$ (MW 502.66):[10e] C, 42.92; H, 5.80; N, 16.69; Cl, 7.04. Found: C, 44.19; H, 6.00; N, 16.73; Cl, 6.95. MS: *m/z* 505. IR: $\tilde{\nu}$(BH) = 2545 cm^{-1}, $\tilde{\nu}$(MoO) = 944 cm^{-1}, $\tilde{\nu}$(MoCl) = 336 cm^{-1}.

LMoOCl(S^{n}Pr) (10). The crude product was dissolved in benzene, and the solution was chromatographed on silica gel with benzene. The compound was eluted as a dark green band, evaporated to dryness in vacuo. The yield was 57%. Anal. Calcd for $C_{18}H_{29}BClN_6OSMo$ (MW 519.73): C, 41.60; H, 5.61; N, 16.17; Cl, 6.82; S, 6.17. Found: C, 42.38; H, 5.62; N, 16.23; Cl, 6.97; S, 6.10. MS: *m/z* 521. IR: $\tilde{\nu}$(BH) = 2552 cm^{-1}, $\tilde{\nu}$(MoO) = 943 cm^{-1}, $\tilde{\nu}$(MoCl) = 325 cm^{-1}.

LMoOCl(S^{i}Pr) (11). The purification process for this compound is similar to that for compound **10**. The yield was 66%. Anal. Calcd for $C_{18}H_{29}BClN_6OSMo$ (MW 519.73): C, 41.60; H, 5.62; N, 16.17; Cl, 6.82; S, 6.17. Found: C, 42.25; H, 5.5; N, 16.07; Cl, 6.93; S, 6.02. MS: *m/z* 521. IR: $\tilde{\nu}$(BH) = 2545 cm^{-1}, $\tilde{\nu}$(MoO) = 940 cm^{-1}, $\tilde{\nu}$(MoCl) = 334 cm^{-1}.

Physical Measurements. Mass spectra were obtained with a Finnigan 3300 quadrupole gas chromatographic/mass spectrometer (GC/MS) with an INCOS data system or a Hewlett Packard 5988A quadrupole GC/MS with a RTE-6 data system. Infrared spectra of the powdered samples (pellets containing 0.5 mg of compound and 80 mg of KBr) were taken on a Perkin-Elmer PE 983 spectrometer. Electron paramagnetic resonance spectra of the fluid solutions (at room temperature) or frozen glasses in toluene (at liquid-nitrogen temperature) were recorded at

(4) Chang, C. S. J.; Collison, D.; Mabbs, F. E.; Enemark, J. H. *Inorg. Chem.* **1990**, *29*, 2261–2267.
(5) Chang, C. S. J.; Rai-Chaudhuri, A.; Lichtenberger, D. L.; Enemark, J. H. *Polyhedron* **1990**, *9*, 1965–1973.
(6) Preliminary reports of a portion of this work have been presented at the First Biennial Symposium on Materials Characterization, Tucson, AZ, March 12–13, 1990.
(7) Bercaw, J. R.; Garrett, A. B. *J. Am. Chem. Soc.* **1956**, *78*, 1841–1843.
(8) Trofimenko, S. J. *J. Am. Chem. Soc.* **1967**, *89*, 6288–6294.
(9) Cleland, W. E., Jr.; Barnhart, K. M.; Yamanouchi, K.; Collison, D.; Mabbs, F. E.; Ortega, R. B.; Enemark, J. H. *Inorg. Chem.* **1987**, *26*, 1017–1025.

(10) Elemental analyses indicate that several samples are partially solvated; the solvent contents that best fit the analyses are as follows: (a) Calcd for **2**·$^1/_3$C$_6$H$_6$: C, 45.73; H, 5.76; N, 16.00; S, 6.10. (b) Calcd for **3**·$^1/_6$C$_6$H$_6$: C, 45.64; H, 5.94; N, 15.97; S, 6.09. (c) Calcd for **4**·$^2/_5$C$_5$H$_{10}$: C, 48.18; H, 6.16; N, 16.05. (d) Calcd for **5**·$^1/_3$C$_6$H$_6$: C, 45.42; H, 5.81; N, 15.13; S, 11.55. (e) Calcd for **8**·$^1/_6$C$_5$H$_{10}$: C, 44.17; H, 5.85; N, 16.27; Cl, 6.86.

X-band frequencies with a Varian E-3 spectrometer. All of the EPR spectra were calibrated with DPPH standard. Electronic absorption spectra were obtained on an IBM 9420 spectrophotometer or an Olis 4300S modified Cary 14 UV/vis/near-IR spectrophotometer. Cyclic voltammetric measurements were performed in acetonitrile solutions (ca. 1–4 mM) over the potential range +2.0 to −2.0 V with 0.1 M tetra-*n*-butylammonium tetrafluoroborate as supporting electrolyte. The electrochemical cell employed a platinum-disk electrode as the working electrode, a platinum-wire counter electrode, and a Hg/Hg_2Cl_2 reference electrode (SCE). All scans were recorded on an IBM EC 225 voltammetric analyzer equipped with an IBM 7424 MT X-Y-T recorder. Potentials were calibrated by addition of ferrocene as an internal standard after each experiment so that errors arising from junction potentials could be minimized.[11] Potentials are reported with respect to the SCE. The peak-to-peak separation (ΔE_p) between the cathodic and anodic peaks and the ratio of the anodic and cathodic currents (i_{pa}/i_{pc}) were used as criteria for the reversibility of the redox processes. Controlled-potential coulometry of compounds in dichloromethane solution was performed on a Model 680 computing coulometer (The Electrosynthesis Co., Inc., East Amherst, NY) in a three-compartment cell (separated with a frit between each compartment) with a graphite working electrode, a platinum-flag auxiliary electrode, and a $Ag/AgNO_3/CH_3CN$ reference electrode with a Vycor tip. The potentials for the bulk electrolysis in dichloromethane were performed about 0.2 V past the cathodic-peak potential of the appropriate cyclic voltammogram of each complex in this system.

Results and Discussion

All of the complexes **1–11** possess at least one chiral center; complexes **2–5** contain more than one chiral center and hence could exhibit diastereomers. However, none of the measurements for complexes **2–5** obtained from EPR spectroscopy and cyclic voltammetry show any evidence for distinguishable diastereomeric pairs.

Mass Spectroscopy. The mass spectra support the mononuclear formulation for these complexes. The mass number for each compound reported in the Experimental Section refers to the peak of maximum intensity within the multiplet around the parent ion peak. A peak of m/z 411 (the base peak for complexes **1–8**) is observed in every compound, corresponding to the formation of the [LMoO] cation. For compounds **6–8**, the peak for the cation of [LMoOCl] at m/z 446 is observed. For compounds **9–11**, both the peaks for the cations of [LMoO(SR)] and [LMoOCl] are found. In addition, all complexes **1–11** exhibit features at m/z 95 and 96, which can be assigned to a displaced pyrazole ring.

Infrared Spectra. The frequencies for the stretching vibration of MoO multiple bonds span a narrow range, 928–947 cm^{-1}, which is lower than that of $LMoOCl_2$ ($\tilde{\nu}$(Mo=O) = 961 cm^{-1}). This result suggests that the better π-donor ligands located cis to the terminal oxo ligand can compete with the available vacant d_π (mainly d_{xz} and d_{yz}) orbitals of the metal atom, thereby reducing the bond order between the molybdenum atom and the terminal oxygen atom.[12] This behavior is not unexpected and is found in many other complex systems. Garner reported that a shift in $\tilde{\nu}$(Mo=O) to higher frequency was observed as the electron-withdrawing nature of the substituents increased for complex series of $[MoO(SR)_4]^-$ (R = C_6H_5, $C_{10}H_7$, 4-$CH_3C_6H_4$, 3-ClC_6H_4, 4-FC_6H_4, 2,6-$Cl_2C_6H_3$, C_6F_5).[13] In addition, the Mo–O stretch of $[MoO(SR)_4]^-$ is lower than that of $[MoOX_4]^-$ (X = Cl, Br, I), corresponding to the poorer π-donor ability of halide versus alkanethiolato ligands.[14]

Electronic Absorption Spectra. The data from the electronic spectra of the complexes in acetonitrile solution in the range of 400–900 nm are summarized in Table I. The absorption bands below 400 nm are mainly intraligand charge-transfer transitions, with high intensities that preclude the location of any possible d → d transition. Near-infrared spectroscopy (900–2000 nm) exhibits only weak overtone peaks of CH vibrations, and no transition bands in this region can be assigned to a molybdenum chromophore for complexes with sulfur donor atoms.

Table I. Electronic Absorption Data in the Range 400–900 nm[a]

compd	$\tilde{\nu}$, 10^3 cm^{-1}	λ, nm	ε, $L \cdot mol^{-1} \cdot cm^{-1}$
1	16.58	603	145[b]
2	16.56	604	134
3	16.75	597	162
4	15.22	657	22
	18.66	536	23
5	11.75	851	211
	15.36	651	259
6	13.05	766[c]	21
7	12.99	770	24
8	12.87	777	22
9	15.60	641	532[d]
10	15.55	643	1036
11	15.46	647	1004

[a] In CH_3CN solution. [b] The value reported in the previous literature is 130 (measured in 1,2-dichloroethane; see ref 9). [c] The value reported in the previous literature is 775 nm (see ref 9). [d] The value reported in the previous literature is 410 (see ref 9).

In complexes **4** and **6–8**, the extinction coefficients (ε) of the absorption bands in the range 400–900 nm are smaller than 30 $L \cdot mol^{-1} \cdot cm^{-1}$. Consequently, these absorption bands are ascribed to ligand-field transitions that are mainly $d_{xy} \rightarrow d_{xz}$ (and/or d_{yz}) in character. In contrast, in complexes **9–11**, the values of ε for the lowest energy transition are greater than 500 $L \cdot mol^{-1} \cdot cm^{-1}$ and can be ascribed to ligand-to-metal (probably sulfur-to-molybdenum) charge-transfer transitions. No d → d transitions can be identified presumably because they are obscured by the charge-transfer transition bands. Similar absorptions have been reported in other monomeric monooxomolybdenum(V) complexes. For example, in $[Et_4N][MoO(SAr)_4]$, λ_{max} (ε) = 598 nm (660) and 610 nm (710) for Ar = phenyl and *p*-tolyl, respectively.[15] Nevertheless, the values of ε of these transitions are not as high as commonly observed for charge-transfer transition bands in other mononuclear monooxomolybdenum(V) complexes, like *cis*-$MoOCl(C_8H_{18}N_2S_2)$ (λ_{max} = 526 nm, ε = 2.65 × 10^3) and *cis*-$MoOCl(C_{10}H_{22}N_2S_2)$ (λ_{max} = 510 nm, ε = 2.10 × 10^3).[16] The visible absorption spectra of resting and active xanthine oxidase show a shoulder at 580 nm, which is suggested to arise from the presence of a molybdenum chromophore,[17,18] and model compounds indicate that sulfur-to-molybdenum charge-transfer transitions can occur in this range.[15] The values of ε of the absorption bands in complexes **1–3** and **5**, which contain at least one sulfur donor atom in their bidentate ligands, are in the range 130–260. Since ligands containing soft donor atoms have been shown to facilitate charge-transfer transition in some oxomolybdenum(V) complexes,[4,9,19] substantial charge-transfer character is also attributed to the absorption bands in complexes **1–3** and **5**.

All of these complexes, except for **4** and **5**, give a single absorption band in the range 400–900 nm. For complexes **4** and **5**, there are two absorption bands, which have similar extinction coefficients and which are separated by 3440 and 3610 cm^{-1}, respectively. Similar results are also observed in the other five-membered chelated diolato and dithiolato complexes.[4]

From Table I, the λ_{max} values of the lowest energy transitions for complexes **1–3** in acetonitrile solution are almost identical, indicating that introducing methyl groups to the five-membered chelate rings does not affect the energy gap of the first electronic

(11) Gang'e, R. R.; Koval, C. A.; Lisensky, G. C. *Inorg. Chem.* **1980**, *19*, 2854–2855.
(12) Nugent, W. A.; Mayer, J. M. *Metal-Ligand Multiple Bonds*; Wiley: New York, 1988.
(13) Ellis, S. R.; Collison, D.; Garner, C. D. *J. Chem. Soc., Dalton Trans.* **1989**, 413–417.
(14) Garner, C. D.; Hill, L.; Howlader, N. C.; Hyde, M. R.; Mabbs, F. E.; Routledge, V. I. *J. Less-Common Met.* **1977**, *54*, 27–34.
(15) Boyd, I. W.; Dance, I. G.; Murray, K. S.; Wedd, A. G. *Aust. J. Chem.* **1978**, *31*, 279–284.
(16) Spence, J. T.; Minelli, M.; Kronek, P.; Scullane, M. I.; Chasteen, N. D. *J. Am. Chem. Soc.* **1978**, *100*, 8002–8004.
(17) Massey, V.; Brumby, P. E.; Komai, H.; Palmer, G. *J. Biol. Chem.* **1969**, *244*, 1682–1691.
(18) Garbett, K.; Gillard, R. D.; Knowles, P. F.; Stangroom, J. E. *Nature* **1967**, *215*, 824–828.
(19) Kay, A.; Mitchell, P. C. H. *J. Chem. Soc. A* **1970**, 2421–2428.

Table II. Electronic Paramagnetic Resonance Data[a]

compd	g_1	g_2	g_3	$\langle g \rangle$[b]	$\langle A \rangle$[c]
1	1.990	1.962	1.925	1.960	39.3
2	1.989	1.963	1.925	1.957	38.8
3	1.988	1.965	1.926	1.959	38.4
4[d]	1.974	1.962	1.907	1.949	38.7
5	2.015	1.972	1.940	1.978	36.7
6	1.970	1.944	1.908	1.940	46.4
7	1.968	1.945	1.906	1.939	45.3
8	1.966	1.943	1.904	1.940	46.8
9	1.999	1.949	1.927	1.959	42.0
10	1.999	1.951	1.927	1.959	42.3
11	1.995	1.948	1.924	1.960	42.5

[a] The measurements at X-band frequencies fall in the ranges $g \pm 0.002$ and $A \pm 1.0 \times 10^{-4}$ cm^{-1}. [b] Isotropic g values obtained at room temperature. [c] ^{95,97}Mo, $\times 10^{-4}$ cm^{-1}. [d] Mean values of measurements obtained from X- and Q-band frequencies.

excitation transition. Complex **5** shows a red shift, approximately 300 and 360 cm^{-1} for the first and second transitions, individually, from LMoO[S-$(CH_2)_2$-S].[4] Red shifts are also observed in the d → d transitions of the diolato complexes with five-membered chelate rings. Complex **4**, which contains a dimethyl-substituted diolato chelate ring, shows d → d transitions that exhibit red shifts of 280 and 105 cm^{-1}, respectively, from those of LMoO[O-CHMeCH$_2$-O] and 400 and 280 cm^{-1}, respectively, from those of LMoO[O-$(CH_2)_2$-O].[4] Similar results are observed for LMoO[O-$(CH_2)_2$-O] and its monoalkyl-substituted complexes LMoO[O-CHRCH$_2$-O] (R = Me, Et, ^{n}Pr, ^{t}Bu); the d → d transitions of the monoalkylated complexes show red shifts of 120–260 and 180–390 cm^{-1} for the first and second transitions, respectively, from those of LMoO[O-$(CH_2)_2$-O].[4]

For monoalkoxo and monoalkanethiolato complexes, both series show small red shifts in their lowest energy transitions, of about 90 ± 30 and 70 ± 20 cm^{-1} for complex series **6–8** and **9–11**, respectively, with an increase of each methylene unit in the alkyl chain. The red shift in these two complex series is quite small. However, this result may still indicate that a minor variation in the electron-releasing ability of the substituents on the monodentate ligands slightly affects the energy of the ligand-field or of the charge-transfer transition in these complex systems.

EPR Spectra. Table II records the isotropic and anisotropic g values and isotropic ^{95,97}Mo hyperfine parameters, $\langle A \rangle$, for each complex. The EPR spectra of these complexes are highly dependent upon the type of the donor atom in the ligands coordinated to the molybdenum atom in the $[LMoO]^{2+}$ core. A correlation diagram between parameters of $\langle g \rangle$ and $\langle A \rangle$ shows that the isotropic and anisotropic g values increase with the number of sulfur atoms in the chelate rings and with the replacement of oxygen by sulfur in the monodentate ligands.[4] The data show in Table II clearly indicate that one of the principal g values will be always greater than 1.987 when one sulfur atom is present in the coordination sphere. For the complex series with chelate rings, both g_1 and g_3 increase in the order **4** < **1–3** < **5**. The value of g_2 for complex **4** is close to that of complexes **1–3** but is smaller than that of complex **5**. Similar results for the anisotropic g_i value are also observed between the monoalkoxo and monoalkanethiolato complexes.

Spin–orbit coupling between the electron spin and the orbital angular momenta results in a deviation of the g value from a free-electron value (g_e). Several mechanisms may contribute to this deviation in the present complex system containing oxygen or sulfur donor atoms.[20] Equation 1 may be used to describe the

$$g_i = g_e - \sum\left[\frac{\zeta_{Mo}F}{\Delta E_{LF}}\right] + \sum\left[\frac{\zeta_{Mo}G}{\Delta E_{CT}}\right] \qquad (1)$$

g value observed in complexes **1–11**.[4,9,21–23] Here each summation contains all appropriate excited-state wave functions; ζ_{Mo} is the one-electron spin–orbit coupling constant for an unpaired electron in a d orbital of the molybdenum atom; F and G are terms containing spin–orbit coupling contributions from the ligands and mixing of ground and appropriate excited states and may be expected to be relatively insensitive to delocalization of unpaired electrons; ΔE_{LF} is the energy associated with the ligand-field transition; ΔE_{CT} is the energy associated with a charge-transfer transition from the filled ligand orbitals to the half-filled HOMO. In complexes **4** and **6–8**, the $\sum[\zeta_{Mo}F/\Delta E_{LF}]$ term dominates due to lack of low-energy charge-transfer transitions, and the observed g values will be smaller than g_e. However, the decrease of the g value due to the ligand-field term can be compensated by the positive $\sum[\zeta_{Mo}G/\Delta E_{CT}]$ term, as observed in complexes **1–3**, **5**, and **9–11**. Therefore, the g values decrease upon replacement of a sulfur donor atom by an oxygen donor atom in a complex with otherwise identical ligands and similar stereogeometry.

Table III. Electrochemical Data[a,b]

	Mo(V) + e$^-$ ⇌ Mo(IV)			
compd	$E_{1/2}$, V	ΔE_p, mV	i_{pa}/i_{pc}	n[c]
1	−0.808	96	0.98	1.15
2	−0.828	82	1.01	1.12
3	−0.856	92	1.02	1.18
4	−1.242	84	1.01	1.12
5	−0.417	65	1.01	1.09
6	−0.909	78	0.93	1.06
7	−0.928	66	0.93	0.98
8	−0.944	130	0.85	1.13
9	−0.489	66	0.95	0.94
10	−0.500	62	1.01	0.99
11	−0.513	114	0.96	0.92
$LMoOCl_2$	−0.329	64	0.97	1.13

[a] Conditions: cyclic voltammetry, platinum-disk working electrode, 1–4 mM in CH_3CN, 0.1 M Bu_4NBF_4 as supporting electrolyte. [b] Potentials reported vs $Hg/HgCl_2$ reference electrode, 25 °C. [c] Number of electrons transferred for each molybdenum atom. Conditions: controlled-potential coulometry in CH_2Cl_2, graphite working electrode, platinum-flag auxiliary electrode, $Ag/AgNO_3/CH_3CN$ reference electrode.

The $\langle A \rangle$ parameters for the complexes with sulfur donors are smaller than the $\langle A \rangle$ values for the complexes with oxygen donors, indicating greater delocalization of the unpaired electron from the d orbital of the molybdenum atom onto the sulfur donor atom. This result is also consistent with a higher degree of convalency for the Mo–S bond and reflects the ability of sulfur-containing ligands to facilitate charge-transfer transitions in the electronic absorption spectra.

The spectra obtained from the frozen-glass state show that complexes **1–4** and **6–8** appear to have rhombic symmetry, whereas the spectra for complexes **5** and **9–11** exhibit approximate axial symmetry. In most cases, the isotropic g values obtained directly from fluid-solution measurements at room temperature agree well with $\sum g_i/3$ obtained by direct measurement from the frozen-solution EPR spectra.

Electrochemistry. Cyclic voltammetry and controlled-potential coulometry are used to investigate the electrochemical behavior of the complexes, and the data are reported in Table III. In the potential window of +2.0 V to −2.0 V, only one well-defined quasi-reversible one-electron-transfer reduction wave is observed for each complex, and this wave is assigned to the mononuclear monooxomolybdenum(V/IV) couple. No oxidation wave, corresponding to formation of the analogous mononuclear monooxomolybdenum(VI) oxidation state, can be observed in the present complexes. The wide range of the reduction potentials (ca. 0.83 V) of these complexes indicates the sensitivity of the reduction potential of the $[LMo^VO]^{2+}$ core to the nature of the remaining ligands.

(20) Young, C. G.; Enemark, J. H.; Collison, D.; Mabbs, F. E. *Inorg. Chem.* **1987**, *26*, 2925–2927.
(21) Glarum, S. H. *J. Chem. Phys.* **1963**, *39*, 3141–3144.
(22) Garner, C. D.; Hillier, I. H.; Mabbs, F. E.; Taylor, C.; Guest, M. F. *J. Chem. Soc., Dalton Trans.* **1976**, 2258–2261.
(23) Garner, C. D.; Mabbs, F. E. *J. Inorg. Nucl. Chem.* **1979**, *41*, 1125–1127.

Four classes of complexes have been studied here: (a) 2-mercaptoethanolato chelate complexes **1–3**, (b) the diolato and dithiolato complexes **4** and **5**, (c) the monoalkoxo complexes **6–8**, and (d) the monoalkanethiolato complexes **9–11**. For the complex series in class a, the half-wave reduction potential shifts to more negative values by 24 ± 4 mV with each increase of one methyl substituent on the five-membered chelate ring. A plot of the reduction potentials ($E_{1/2}$) versus the number of methyl groups (m) gives a line with a correlation coefficient 0.995, as shown in eq 2.

$$E_{1/2} = -0.024m - 0.807 \quad (2)$$

In class b, complex **4** shows a more negative reduction potential compared with those of LMoO[O–CH(Me)CH_2–O] and LMoO[O–$(CH_2)_2$–O];[4] the individual shifts are 67 and 82 mV, respectively. The correlation line between $E_{1/2}$ and m is

$$E_{1/2} = -0.0410m - 1.151 \quad (3)$$

with a correlation coefficient of 0.939. The slope of eq 3 is greater than that of eq 2, indicating that the reduction potentials of the diolato complexes are more sensitive to the number of methyl substituents on the chelate rings than the 2-mercaptoethanolato chelate complexes of class a. The half-wave reduction potential for complex **5** is 50 mV more negative than that of the unsubstituted dithiolato complex LMoO[S–$(CH_2)_2$–S].

For complexes in class c, the plot between $E_{1/2}$ and the number of methylene units (n) in the alkoxide chain gives a line with a correlation coefficient of 0.999:

$$E_{1/2} = -0.0175n - 0.910 \quad (4)$$

The slope is smaller than those of both eqs 2 and 3 and is consistent with the prediction from a comparison of the PES between a series of diolato and dialkoxo complexes.[5]

For the complexes in class d, the average shift in the reduction potential with an increase of one methylene unit is −11 mV. The difference in behavior of 1- and 2-propanethiolato complexes (**10** and **11**) is not unusual, since the ligands have different inductive effects.

It is well-known that ligand substituents may affect the electrochemical potential by disturbing the π-bonding ability of the ligand.[24] Here, the systematic variation of substituents, which possess different inductive effects, introduces an electronic perturbation to the reduction processes for the complexes. However, such a "tuning" of the potential with changes in the number of the methylene units in the monoalkoxo complexes, **6–8**, or monoalkanethiolato complexes, **9–11**, is slightly smaller than the corresponding potential changes with the number of substituent methyl groups in the chelate complexes, **1–3**. This phenomenon may be due to a decrease in the inductive effect with increasing distance from metal center.

Table III also shows that the half-reduction potential of the complexes containing sulfur donors is at least 430 mV more positive than for the complexes with oxygen donors. This result is similar to those for other complex systems.[4,9,25-31]

The reduction potentials of the Mo(V)/Mo(IV) couple for the present complexes suggest that the ligands, when coordinated to the $[LMoO]^{2+}$ core, enhance the stability of the Mo(IV) oxidation state in the order **5** > **9** > **10** > **11** > **1** > **2** > **3** > **6** > **7** > **8** > **4**. This overall trend is consistent with the common concept of hard–soft–acid–base, since the sulfur atom is a soft donor and the Mo(IV) oxidation state should be softer than the Mo(V) state.

The results from EPR spectroscopy, cyclic voltammetry, and controlled-potential coulometry for complexes **1–11** indicate that the highest occupied molecular orbital (HOMO) is mainly molybdenum $4d_\pi$ orbital in character. In addition, the contribution to the half-wave reduction potential from the inductive effect of each ligand substituent is *additive* with the increase of the number of methyl groups on the chelate rings or methylene groups in the monodentate ligands (vide ante). Therefore, the observed shifts of the half-wave reduction potentials may be rationalized as reflecting changes in the ligand-to-metal π-interaction of the filled donor atom p_π orbitals with the half-filled d_π orbital (d_{xy}) of the molybdenum atom.[32] In these complexes, the inductive effects of methyl and methylene groups destabilize the HOMO, and the complexes become more difficult to reduce in acetonitrile solution. In addition, from Table III, it is clear that complexes **1–11** are more difficult to reduce than $LMoOCl_2$, consistent with the better π-bonding ability of sulfur- and oxygen-containing ligands (vide ante) compared to chloride.[5]

Several other measurements support the above interpretation: (i) The gas-phase He I PES for several diolato and dialkoxo complexes show that the ionization potentials for electrons in the orbitals mainly localized in the oxo and pyrazolylborate ligands do not differ significantly from complex to complex, consistent with the nonbonding character of these orbitals. However, the ionizations, which are mainly from p_π orbitals of the donor atoms on the diolato ligands and from the HOMO, are stabilized and destabilized, respectively,[5] supporting a ligand-to-metal p_π–d_π interaction. (ii) The parallel structural parameters for $[LMoO]^{2+}$ between the complexes $LMoO(NCS)_2$ and $LMoO(N_3)_2$ are similar.[33] A similar result is also observed for $LMoO(SPh)_2$,[9] $LMoO(OPh)_2$,[34] and $LMoO(O\text{-}C_6H_4\text{-}X)_2$ (X = CH_3, Cl).[35] Therefore, the $[LMoO]^{2+}$ core can be assumed to have similar electronic arrangements among complexes. Consequently, the differences in reduction potential may reflect the perturbation by the inductive effects of the substituents in each complex. Other factors such as the solvation energy will probably be similar for the complexes described here, which possess closely related coordination geometries.

Conclusions

This work shows that a systematic variation of the inductive effects of ligands that coordinate to the $[LMoO]^{2+}$ core in a series of oxomolybdenum(V) complexes with similar chemical environments can perturb the spectroscopic and electrochemical behaviors. However, unlike the variation of the sizes of chelate rings,[4] a change in the number of methyl groups in complexes **1–5** or the methylene units in complexes **6–11** introduces only minor perturbations.

The half-filled HOMO is the orbital that is responsible for the redox behavior observed in the electrochemistry. The stronger the interaction between the p_π orbitals of the ligand donor atoms and the d_π orbital (d_{xy}) of the molybdenum atom, the more the energy of the HOMO will be raised, making the complex more difficult to reduce. Destabilization of the HOMO will also decrease the energy gap between the HOMO, which is mainly $4d_{xy}$ in character, and the other unoccupied metal 4d orbitals, leading to a red shift in the d → d transition, as observed in both the diolato

(24) Buckingham, D. A.; Sargeson, A. M. In *Chelating Agents and Metal Chelates*; Dwyer, F. P., Meller, D. P., Eds.; Academic Press: New York, 1964; pp 237–282.
(25) Bond, A. M.; Martin, R. L.; Masters, A. F. *Inorg. Chem.* **1975**, *14*, 1432–1435.
(26) Bond, A. M.; Martin, R. L.; Masters, A. F. *J. Electroanal. Chem. Interfacial Electrochem.* **1976**, *72*, 187–196.
(27) Ott, V. R.; Swieter, D. S.; Schultz, F. A. *Inorg. Chem.* **1977**, *16*, 2538–2545.
(28) Schultz, F. A.; Ott, V. R.; Rolison, D. S.; Bravard, D. C.; McDonald, J. W.; Newton, W. E. *Inorg. Chem.* **1978**, *17*, 1758–1765.
(29) Taylor, R. D.; Street, J. P.; Minelli, M.; Spence, J. T. *Inorg. Chem.* **1978**, *17*, 3207–3211.
(30) Berg, J. M.; Holm, R. H. *J. Am. Chem. Soc.* **1985**, *107*, 917–925.
(31) Boyd, I. W.; Spence, J. T. *Inorg. Chem.* **1982**, *21*, 1602–1606.
(32) A reviewer suggested that ligand substituents may also affect electrochemical potentials by inductive effects transmitted through σ-bonding pathways. We cannot rule out this possibility, but a σ-pathway seems less important for the present complexes because the d_σ orbitals of the molybdenum atom are empty.
(33) Roberts, S. A.; Ortega, R. B.; Zolg, L. M.; Cleland, W. E., Jr.; Enemark, J. H. *Acta Crystallogr.* **1987**, *C43*, 51–53.
(34) Kipke, C. A.; Cleland, W. E., Jr.; Roberts, S. A.; Enemark, J. H. *Acta Crystallogr.* **1989**, *C45*, 870–872.
(35) (a) Chang, C. S. J.; Pecci, T. J.; Carducci, M. D.; Enemark, J. H. Manuscript in preparation. (b) Chang, C. S. J.; Pecci, T. J.; Enemark, J. H. Unpublished data.

and monoalkoxo complex series **9-11**.

The substituents on chelate rings and monodentate ligands exhibit different inductive effects, which are responsible for various ligand-to-metal π-interactions among complexes. The π-donor ability of the ligands in complexes **1-11** increases in the following orders: (i) for the 2-mercaptoethanolato chelated complexes, **1** < **2** < **3**; (ii) for the alkoxo complex series, **6** < **7** < **8**; and (iii) for the alkanethiolato complex class, **9** < **10** < **11**. This parallels the electron-releasing tendency of the substituents of the ligands that are coordinated to the $[LMoO]^{2+}$ core.

The observed substituent effects in mononuclear monooxomolybdenum(V) complexes with chelated dithiolato ligands may not be directly applicable to Mo-co, because the cofactor is thought to possess a chelated dithiolene five-membered ring. However, with the exception of the 3,4-toluenedithiolato complex reported previously,[9] repeated attempts to synthesize complexes analogous to **5**, but containing a chelated dithiolene ligand, have been unsuccessful.

Acknowledgment. Support of this research by the National Institutes of Health (Grant GM 37773) is gratefully acknowledged. We acknowledge helpful discussions with Dr. M. A. Bruck, Dr. S. A. Roberts, Dr. K. Yamanouchi, Dr. A. G. Wedd, M. D. Carducci, P. J. Desrochers, and M. J. LaBarre.

Contribution from the Biomedical Chemistry Research Center, Department of Chemistry, University of Cincinnati, Cincinnati, Ohio 45221-0172

Technetium Electrochemistry. 7.[1] Electrochemical and Spectroelectrochemical Studies on Technetium(III) and -(II) Complexes Containing Polypyridyl Ligands[2]

Bruce E. Wilcox[3] and Edward Deutsch*

Received January 26, 1990

The redox properties of a series of technetium(III/II) complexes of the general formula *cis*(*X*),*trans*(*P*)-$[Tc^{III/II}X_2(PR_2R')_2L]^{+/0}$, where X = Cl or Br, PR_2R' = dimethylphenylphosphine or ethyldiphenylphosphine, and L = 2,2′-bipyridine (bpy), 4,4′-dimethyl-2,2′-bipyridine (Me_2bpy), or 1,10-phenanthroline (phen), were investigated in 0.1 M TEAP/acetonitrile by cyclic voltammetry at a platinum-disk electrode. These complexes exhibit diffusion-controlled, 1-equiv Tc(IV)/Tc(III) redox couples in the range 1.044-0.965 V vs SCE and also Tc(III)/Tc(II) redox couples in the range -0.049 to -0.189 V vs SCE. Spectropotentiostatic experiments on three complexes of this class in 0.5 M TEAP/DMF confirm the 1-equiv character of the Tc(III)/Tc(II) couple. $E^{\circ\prime}$ values obtained from these spectropotentiostatic data are consistent with values determined from thin-layer cyclic voltammograms. The Tc(IV)/Tc(III) couple is not reversible on the time scale of the spectropotentiostatic experiment. The electrochemical behavior of Tc(II) complexes of the general formula *trans*(*P*)-$[TcX(PR_2R')_2terpy]^+$, terpy = 2,2′:6′,2″-terpyridine, was also investigated under the same conditions as above. These complexes exhibit diffusion-controlled, 1-equiv Tc(III)/Tc(II) redox couples in the range 0.491-0.440 V vs SCE and Tc(II)/Tc(I) redox couples in the range -1.067 to -1.123 V vs SCE. Spectropotentiostatic experiments on *trans*(*P*)-$[TcCl(PMe_2Ph)_2terpy]^+$ confirm the 1-equiv character of the Tc(III)/Tc(II) couple but show that the Tc(II)/Tc(I) couple is not reversible on the spectropotentiostatic time scale. These electrochemical results are discussed in terms of how Tc redox potentials, and thus the stabilities of various Tc oxidation states, can be controlled by manipulating the properties of the ligands bonded to technetium.

Introduction

We have recently reported the synthesis and characterization of technetium(III)[4] and -(II)[5] complexes of the general formula *cis*(*X*),*trans*(*P*)-$[Tc^{III/II}X_2(PR_2R')_2L]^{+/0}$, where X = Cl or Br, PR_2R' = dimethylphenylphosphine or ethyldiphenylphosphine, and L = 2,2′-bipyridine (bpy), 4,4′-dimethyl-2,2′-bipyridine (Me_2bpy), or 1,10-phenanthroline (phen). The Tc(III) species were prepared by replacement of one halide and one phosphine ligand of the *mer*-$[Tc^{III}X_3(PR_2R')_3]$ starting material by the bidentate bipyridyl ligand. The Tc(II) analogues were prepared in good yield by hydroxide reduction of the Tc(III) analogues in ethanol. During these studies it was observed that slight variations in the ligands dictated the preferred oxidation state of the Tc center. For example, the bromo analogue of *cis*(*X*),*trans*(*P*)-$[Tc^{III/II}X_2(PMe_2Ph)_2bpy]^{+/0}$ is more easily obtained in the Tc(II) state and is not readily isolated in the solid form as a Tc(III) species, whereas the converse is true for the *cis*(*X*),*trans*(*P*)-$[Tc^{III/II}Cl_2(PMe_2Ph)_2(Me_2bpy)]^{+/0}$ pair.

Related Tc(II) complexes of the general formula *trans*(*P*)-$[TcX(PR_2R')_2terpy]^+$, where terpy = 2,2′:6′,2″-terpyridine, have also been synthesized and characterized.[5] They are analogously prepared by replacement of one phosphine and two halide ligands from the *mer*-$[Tc^{III}X_3(PR_2R')_3]$ starting materials, but in this system concomitant reduction of Tc(III) to Tc(II) occurs because of the greater stability of the Tc(II) form.

These qualitative observations suggest that these classes of complexes should exhibit a rich electrochemistry characterized by E° values that depend markedly on the nature of the coordinated ligands. The fact that both the Tc(II) and Tc(III) oxidation states are relatively stable also suggests that these systems should be amenable to spectroelectrochemical analysis. The characterization of these systems by both cyclic voltammetric and spectropotentiostatic methods is herein described.

Abbreviations and Acronyms. Definitions of abbreviations and acronyms used in this paper are as follows: $(acac)_2en$ = *N*,*N*′-ethylenebis(acetylacetone iminato); bpy = 2,2′-bipyridine; $(buac)_2en$ = *N*,*N*′-ethylenebis(*tert*-butyl acetoacetate iminato); CV = cyclic voltammogram; DMF = *N*,*N*-dimethylformamide; depe = $(CH_3CH_2)_2PCH_2CH_2P(CH_3CH_2)_2$; diars = *o*-bis(dimethylarsino)benzene; dmpe = $(CH_3)_2PCH_2CH_2P(CH_3)_2$; dppe = $Ph_2PCH_2CH_2PPh_2$; Et = ethyl; Me = methyl; Me_2bpy = 4,4′-dimethyl-2,2′-bipyridine; Ophsal = *N*-(2-hydroxyphenyl)-salicylideneaminato; OTTLE = optically transparent thin-layer electrode; PDE = platinum-disk electrode; $PEtPh_2$ = ethyldiphenylphosphine; Ph = phenyl; phen = 1,10-phenanthroline; phsal = *N*-phenylsalicylideneaminato; PMe_2Ph = dimethylphenylphosphine; SCE = saturated calomel electrode; TEA = tetraethylammonium ion; TEAP = tetraethylammonium perchlorate; terpy = 2,2′:6′,2″-terpyridine.

Experimental Section

Materials. *Caution*! All references to technetium in this paper are to the specific isotope ^{99}Tc, which emits a low-energy (0.292 MeV) β particle with a half-life of 2.12×10^5 years. When this material is handled in milligram amounts, it does not present a serious health hazard,

(1) Part 6: Kirchhoff, J. R.; Heineman, W. R.; Deutsch, E. *Inorg. Chem.* **1988**, *27*, 3608.
(2) Abstracted from the Ph.D. dissertation of B.E.W., University of Cincinnati, 1987.
(3) Current address: Department of Chemistry, Bloomsburg University, Bloomsburg, PA 17815.
(4) Wilcox, B. E.; Ho, D. M.; Deutsch, E. *Inorg. Chem.* **1989**, *28*, 1743.
(5) Wilcox, B. E.; Ho, D. M.; Deutsch, E. *Inorg. Chem.* **1989**, *28*, 3917.

0020-1669/91/1330-0688$02.50/0